Ultrasoft Colloids

DOI: 10.1002/anie.200906606

Microgel Translocation through Pores under Confinement**

*Grant R. Hendrickson and L. Andrew Lyon**

In applications utilizing synthetic biomaterials, such as drug delivery,[1–4] bioimaging,[5,6] and tissue engineering,[7–11] the material mechanical properties represent an important set of design parameters.[12] Most studies of mechanical properties in biomaterials have focused on how cells interact with or move on surfaces of different rigidity in the context of mechanotransduction[7,10,11] and cell proliferation or differentiation.[8,9] However, few studies have investigated the effects of the mechanical softness of nanoparticles in nano- or microbiological environments. It has been suggested, however, that the softness of nanoparticles may be relevant in processes such as phagocytosis or endocytosis.[13,14] This concept implies that cells are not only affected by the mechanics of large surfaces or interfaces but also by the rigidity of individual nanoparticles. The in vivo performance of nanoparticles is strongly dependent on a variety of biological processes, including lymphatic drainage, endocytosis, extravasation, and kidney filtration. It stands to reason that any process that has a rigid size dependence may also be dependent on the mechanical flexibility of the biomaterial.[15] Therefore, it is necessary to consider mechanics when outlining the nanoparticle size restrictions relevant for certain processes. This aspect might especially be important when the process involves passage through small, well-defined pores, such as in renal filtration.

Renal or glomerular filtration is one of two routes of clearance of biomaterials from the body for particles smaller than 500 nm.[12,15,16] The other clearance route is biliary clearance through the liver; however, in nanomedicine applications biliary clearance is generally bypassed owing to the small particle sizes typically used.[16] Therefore, renal clearance is a desired mechanism of nanoparticle excretion. This mechanism requires passage through approximately 8 nm diameter pores (as defined by endothelial gaps) under a pressure differential of 40 to 80 Torr (0.7 to 1.5 psi).[17–21] Obviously, for most carrier systems these figures of merit are not easily met and require the integration of degradability into the nanoparticle design or rigorous control over small particle sizes.[22–25] In some cases, these modifications may negatively alter drug loading and release, circulation times, cell uptake, and cytotoxicity. Therefore, it may be desirable to develop a carrier system that has the ability to be excreted without additional design complexity. For a hard-sphere system, such as quantum dots, this stipulation implies a strict particle size limit,[26] which may negatively impact payload or may result in clearance through lymphatic drainage.[27] However, soft conformable nanoparticles that are able to deliver a large cargo yet are flexible enough to fit through small pores are a potentially attractive alternative. One example of such a construct is that of hydrogel colloids (i.e. nanogels or microgels), which are nanoparticles that can be dramatically compressed, owing to their significant network flexibility.[28]

Herein we describe the first demonstration of microgel translocation through cylindrical pores under pressure differentials relevant to renal filtration. We observe that microgel particles easily pass through such pores, even when the opening is more than tenfold smaller than the unperturbed microgel diameter. For this study, track-etch membranes were used as the model for pores in the renal system. As shown in Scheme 1, track-etch membranes were placed into gasket-sealed syringe filter holders and placed onto a Luer lock syringe that was enclosed at one end. A fluorescently labeled microgel dispersion was added to the syringe, and approximately 0.5 psi of hydrostatic pressure was applied from a compressed air cylinder to the head space of the syringe. Eluant was then collected and analyzed by steady-state fluorescence.

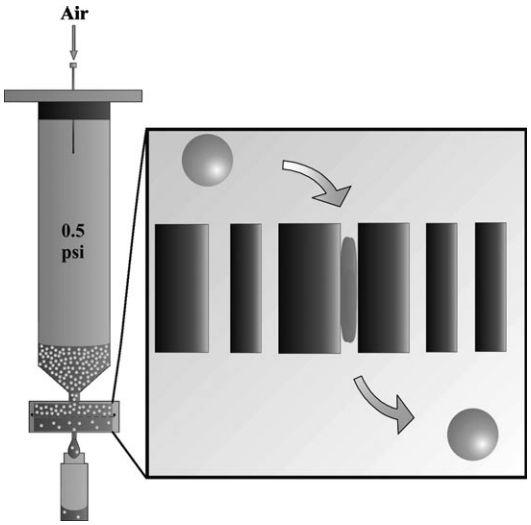

Scheme 1. Scheme of filtration setup and microgel filtration through a track-etch membrane.

The microgels used herein were prepared by copolymerization of *N*-isopropylacrylamide (NIPAm), acrylic acid (AAc, 10 mol%), and 4-acrylamidofluorescein (AFA,

[*] G. R. Hendrickson, Prof. L. A. Lyon
School of Chemistry and Biochemistry and
Petit Institute for Bioengineering and Biosciences
Georgia Institute of Technology, Atlanta, GA 30332-0400 (USA)
Fax: (+1) 404-894-7452
E-mail: lyon@gatech.edu

[**] Financial support from the NIH (1 R01 GM088291-01) is acknowledged. We thank Michael H. Smith for synthesis of the pNIPMAm nanogels.

0.02 mol%) with *N*,*N*′-methylenebis(acrylamide) (BIS) as a cross-linker. The microgel sizes as a function of pH value (pH dependence arises from the AAc comonomer) are shown in Table 1. The 1% cross-linked particles were approximately

Table 1: Hydrodynamic radii (R_h) and swelling properties of microgels at different pH values.[a]

Particle type	R_h [nm] pH 7.4	R_h [nm] pH 3.0	ζ [mV] pH 7.4	ζ [mV] pH 3.0	D%[b]
1% cross-link μGel	570	324	−20.5	−4.1	43
3% cross-link μGel	433	303	−17.3	−3.3	30
88 nm PS	48	46	N/A	N/A	N/A[c]
200 nm PS	101	96	N/A	N/A	N/A[c]

[a] All R_h values were determined by DLS at 25 °C. All ζ potentials were determined by electrophoretic light scattering. N/A = not available. [b] pH-dependent deswelling percentage. [c] No statistical difference in radii between pH 3 and 7 (t test 95%).

1140 nm in diameter fully swollen at pH 7, whereas the 3% cross-linked microgels were smaller (866 nm), as expected owing to the increased cross-linking. Also, the deswelling owing to protonation of the AAc at pH 3 was 43% for the 1% and 30% for the 3% cross-linked microgels. Thus, these two microgel types provided two different sizes with two different pH-dependent compressabilities to investigate the generality of the phenomenon. Note that the difference in cross-linking density should only account for a small difference in swollen-particle elastic modulus (ca. 8 vs. 13 kPa) on the basis of bulk gel literature.[29] More important than the differences in the microgels is the fact that both are significantly larger than the 100 nm track-etch membrane pores. For comparison, volume-conserving, rigid polystyrene beads with diameters of 200 nm (negative control) and 88 nm (positive control) were used in identical filtration experiments.

After filtration, the unfiltered solutions and the resulting eluants were analyzed by steady-state fluorescence spectroscopy, fluorescence microscopy, and bright-field microscopy (Figure 1). The spectra of a 3% cross-linked particle solution before and after filtration and of a buffer solution are shown. Also shown in Figure 1, a more concentrated solution of the same particles was filtered through the 100 nm track-etch membrane, and the solutions were dried on glass cover slips before and after filtration and analyzed by optical microscopy. As the track-etch membranes have an extremely small pore density (100 nm pores: 4 pores μm^{-2}; 10 nm pores: 6 pores μm^{-2}), they do not allow for a high flux of particles, even if the particles are smaller than the pores. Therefore, steady-state fluorescence was used to quantify the polymer mass passed through the filter. The fluorophore loading of the microgels and control polystyrene particles is not equal; however, the unfiltered solutions contained the same amount of polymer in weight percent (wt%). Therefore, calculation of the particle concentration (in wt%) in the filtered solution allowed for fair comparison of particle flux. The fluorescence (corrected for background signal) was converted to polymer concentration by creating standard curves of background-corrected fluorescence to concentration for each particle at each pH value.

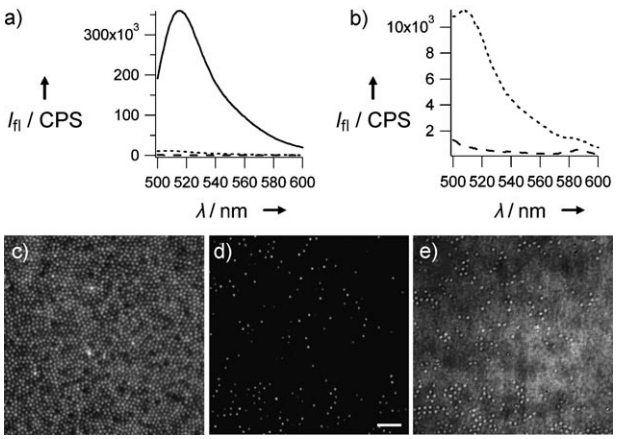

Figure 1. a,b) Fluorescence spectra of a 0.01 wt% solution of 3% cross-linked microgel particles (D_h = 648 nm) before (solid line) and after (dotted line) filtration. The dashed line is pH 7 buffer. A smaller scale version of (a) is shown in (b). c,d) Fluorescence microscopy images before (c) and after (d) filtration and e) a bright-field microscopy image after filtration of the same particles. Scale bar = 5 μm.

The data in Figure 2 display the surprising result that the flux of both microgel types at pH 7 was equal to that of the much smaller PS positive control. A greater difference

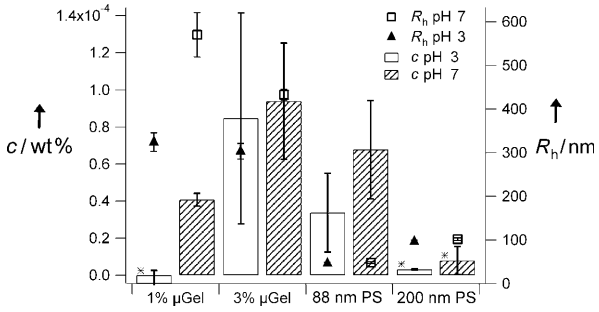

Figure 2. Filtration comparison of 1% and 3% microgels, 88 nm polystyrene, and 200 nm polystyrene particles (0.001 wt%). Error bars represent the uncertainty over three or four filtration experiments. Stars represent statistically significant data at the 95% confidence interval relative to 88 nm polystyrene at pH 7.

between the microgels and the PS control is observed when the overall particle concentration is increased (Figure 3). We tentatively ascribe this concentration dependence to jamming of the PS particles in the pores (see below). It appears, however, that the deformable microgel particles do not display jamming effects at pH 7, presumably owing to their conformational flexibility and Coulombic interparticle repulsion (see Table 1 for measured ζ potentials) during passage.

Two pH values were studied to evaluate the influence of microgel swelling on passage through the pores. At low concentration (Figure 2), the flux of the 1% cross-linked microgel particles at pH 3 is indistinguishable from the background. However, at pH 7 the 1% microgel particles pass readily through the pores, presumably owing to the increased flexibility of the swollen microgel and decreased jamming owing to Coulombic particle–particle repulsion. In

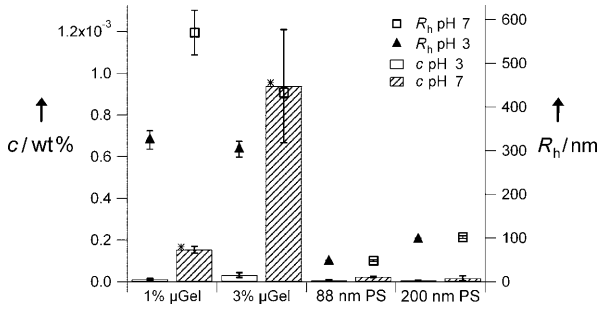

Figure 3. Filtration comparison of 1% and 3% microgels, 88 nm polystyrene, and 200 nm polystyrene particles (0.01 wt%). Error bars represent the uncertainty over three or four filtration experiments. Stars represent statistically significant data at the 95% confidence interval relative to 88 nm polystyrene at pH 7.

the case of the 3% cross-linked microgel particles, there seems to be no difference between the two pH values. This finding is curious, as the two microgel types have similar sizes at pH 3. Therefore, it could be the case that for this concentration and size, a jamming limit is being approached, and subtle differences in microgel modulus and interparticle potential produce large changes in pore passage. This is almost certainly the case when the concentration is increased further (Figure 3, tenfold concentration increase); the observed flux for both microgel types at pH 3 is much lower than that at pH 7. This finding again suggests a jamming effect when the more rigid and less repulsive microgel particles try to fit through the small pores. This effect is emphasized by increasing the concentration another order of magnitude to 0.1 wt% (Figure 4). As the feed concentration increases, only

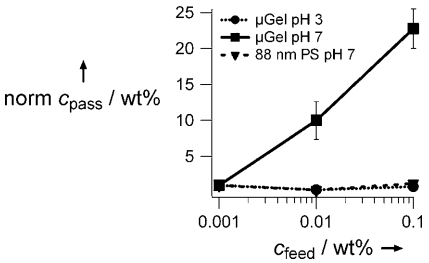

Figure 4. Normalized passed versus feed concentration of 3% cross-linked microgel particles at pH 3 and pH 7 and 88 nm PS at pH 7. The amount passed was normalized to that at the lowest feed concentration.

the flux of the 3% cross-linked particles in their fully swollen state (pH 7) increases, thus suggesting that the PS and deswollen microgels are jamming. It should be noted, however, that when the concentration is increased to 1 wt%, the passage increases for the microgels at both pH 7 and pH 3. The origin of this observation is still under investigation, but given our previous studies of microgel phase behavior at such concentrations,[30–32] it is likely that particle–particle interactions strongly perturb the actual hydrodynamic radii under these conditions. It should also be noted that the particle to pore size ratio of approximately 10:1 appears to be the rough limit for these particles, as larger microgels (diameters greater than 1.5 µm) did not appear to pass through 100 nm pores.

Having observed that pNIPAm–AAc microgels are able to translocate through pores 10 times smaller in diameter, we investigated the generality of this phenomenon to smaller pore sizes with more biologically relevant dimensions. In this case, track-etch membranes with 10 nm pores were used in the same experimental setup (Scheme 1) with the same applied pressure differential of ca. .5 psi. The particles used in this experiment were fluorescent pNIPMAm microgels with a dilute-solution diameter of 116 nm; 88 nm diameter fluorescently labeled polystyrene beads were used as a negative control. The synthesis of the microgels has been published and is discussed briefly in the Experimental Section.[33] As shown in Figure 5, even at these smaller

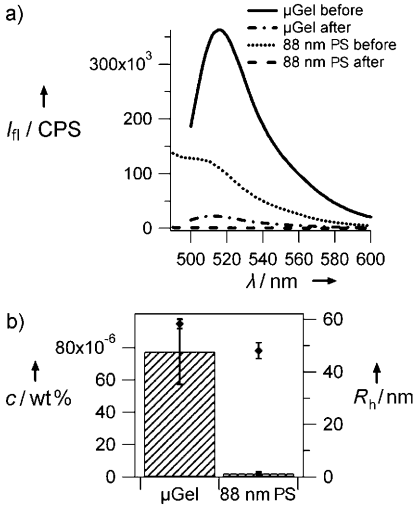

Figure 5. a) Fluorescence spectra of 0.001 wt% solutions of 116 nm microgel particles and 88 nm polystyrene beads before and after filtration through 10 nm pores. The spectra after filtration are averages of four spectra. b) Filtration comparison of 116 nm microgels and 88 nm polystyrene. Diamonds are hydrodynamic radii of particles at pH 7.

dimensions, the microgel particles still pass through the pores (pH 7), while the negative control does not. These data are compelling owing to the similarity in pores size and pressures between those found in the kidney and those used in these experiments. Also, it should be noted that when various fluorescein isothiocyanate dextran samples (MW = 20 or 150 kDa) were used as a positive control, they readily passed through the pores, as expected for a random-chain flexible polymer.

Although the fundamental mechanisms underlying these observations are not understood quantitatively, the biology and physiology community has studied the glomerular filtration rate of macromolecules for many years.[17–20,34,35] It has been found that linear polysaccharides such as dextran have a much greater filtration rate and larger hydrodynamic radius cutoff than do proteins, owing to the rigidity and well-defined secondary structure of the latter.[17]

Also, the soft-matter community has extensively studied the passage of polymers through pores.[36–40] Translocation of a linear polymer through pores or in confined spaces is generally most probable if the polymer can go end-first through the pore (as opposed to folding). Likewise, it has been found that a branched polymer has a higher probability of passage through a pore if more than one chain end can find the pore opening.[15] Therefore, a polymer nanoparticle with low connectivity and many different chain ends may have the conformational freedom to pass through a pore much smaller than its dilute-solution diameter, owing to the high number of energetically degenerate conformations with statistically identical passage probabilities. Also, the compressibility of these particles cannot be underestimated. It has been shown that the combination of polymer and colloidal osmotic pressures in a colloidal crystal of pNIPAm microgels was able to induce the dramatic deswelling of a much larger microgel "defect".[28] In that case the "defect" was compressed to a volume 15 times smaller than its dilute-solution equilibrium volume without imposing any direct mechanical force on the particle. It is therefore not unreasonable to hypothesize that similar microgels could adopt a configuration in which many chains enter the pore under a driving pressure differential, followed by particle collapse or compression and subsequent reswelling as the particle emerges from the other side of the membrane.

In conclusion, we have observed phenomena that illustrate the ability of hydrogel microparticles to pass through pores at least tenfold smaller in size under hydrostatic pressures relevant to renal filtration. This extremely surprising result can be rationalized by considering the extreme softness of these nanoobjects and the conformational flexibility of the polymer chains comprising the particles. Importantly, we have illustrated the generality of the phenomenon to absolute pore sizes that are relevant to renal filtration by using nanogels appropriate in size for injectable drug-delivery formulations. These studies illustrate the importance of considering the mechanical flexibility as a critical design component of nano-biomaterials. This network flexibility and compressibility of microgels is not only interesting in terms of their performance as biomaterials for drug delivery but is also of fundamental interest, as soft-colloid physics has become a vibrant field of study. Indeed, both the fundamental physics of microgel softness and the biological impacts thereof have been and continue to be an active area of investigation within our research group.

Experimental Section

Materials: Monomers *N*-isopropylacrylamide (NIPAm; Aldrich) and *N*-isopropylmethacrylamide (NIPMAm) were recrystallized from hexanes (Fisher Scientific) before microgel synthesis. The fluorescent monomer 4-acrylamidofluorescein (AFA) was synthesized according to the literature procedure.[41] Cross-linker *N*,*N*′-methylenebis(acrylamide) (BIS; Aldrich), ammonium persulfate (APS; Aldrich), and acrylic acid (AAc; Fluka) were all used as received. The polystyrene standards (Duke Scientific) were diluted in a 0.003 wt% surfactant (sodium dodecyl sulfate (SDS; Aldrich)) solution. The track-etch membranes were purchased from Sterlitech (Kent, WA). The pH 7 buffer was a 10 mM (IS = 100 mM) phosphate buffer and the pH 3 buffer was a 10 mM (IS = 100 mM) formate buffer. All water used in the experiments was purified to 18 mΩ (Barnstead E-pure system).

Synthesis: The larger microgels were synthesized by precipitation polymerization of NIPAm, BIS (1 or 3 mol%), AFA (0.02 mol%), and AAc (10 mol%) with a total monomer concentration of 100 mM in 100 mL. All components were dissolved in distilled, deionized water and stirred under a nitrogen purge while being heated to 68 °C. Then APS (0.01 mM) was added to initiate the reaction. The reaction mixture was allowed to stir under nitrogen at 68 °C overnight. For synthesis of smaller microgel particles, NIPMAm was used with BIS and AFA in the same manner, except 8 mM SDS was added to stabilize the particles, the syntheses were performed at 70 °C, and 8 mM APS was used.[33] All particle solutions were filtered and purified by centrifugation. The samples were then freeze-dried for storage.

Size characterization: Dynamic light scattering (DLS) was used to determine the hydrodynamic radius (R_h) at different pH values, as described earlier.[42,43] A Wyatt Technologies DynaPro plate reader DLS instrument was used with a laser wavelength of 830 nm. Scattering intensity fluctuations were detected for 10 s per reading by an avalanche photodiode at an angle of 158° (back-scattering) from the incident laser. Dynamics software (Wyatt Technologies Corp.) was used to calculate and fit an autocorrelation function plotted from the random fluctuations in scattering intensity. These fits of the autocorrelation functions were used to calculate the diffusion coefficients and then, through the Stokes–Einstein equation, the R_h values. The plate reader DLS provided the opportunity to use small volumes (50 μL) of particle solution and to run different aliquots in series without further sample preparation.

Zeta potential measurements were carried out in 5 mM ionic strength 4-(2-hydroxyethyl)-1-piperazineethanesulfonic acid (HEPES, pH 7.4) and formate (3.0) buffers by electrophoretic light scattering with a Malvern Instruments Zetasizer.

Filtration experiments: Syringes (30 mL) were used for the filtration experiments by removing the plunger. Epoxy was used to seal a septum stopper in the top of the syringe. A manufacturer-supplied, Luer lock membrane holder was used to hold the 25 mm radius membranes at the end of the syringe. The holders and syringes were sonicated and rinsed with a dilute Alconox solution and distilled, deionized water before assembly and use. After the syringe was vertically clamped, particle solution (ca. 4 mL) was injected through the septum at the top of the syringe. Finally, a needle attached to a step-down (0–15 psi) regulator was placed into the septum to control the hydrostatic pressure. Approximately 2 mL particle solution was collected, which took anywhere from 4 to 8 h for the 100 nm pore experiments and 24 to 48 h for the 10 nm pore experiments. After collection, all solutions were analyzed on a steady-state fluorescence spectrometer (Photon Technology International) equipped with a Model 814 PMT photon-counting detector. For all microgels containing fluorescein, the excitation wavelength was set to 490 nm and emission was detected between 500 and 600 nm. For the polystyrene standards, excitation was set to 468 nm and emission was collect from 480–600 nm based on the literature from the manufacturer. Then the fluorescence at peak maximum [515 (μGels) or 508 nm (PS)] was recorded. Readings of particles in pH 3 buffer were collected by spiking an aliquot of sample (0.5 mL) with 100 mM pH 9 borate buffer (50 μL) to raise the pH value to approximately pH 8 so that fluorescence would not be quenched. All data was analyzed by a q test, and outliers outside the 95% confidence interval were removed from the data set. Also, the stars in the data sets represent data that is statistically different from the 88 nm PS control at a 95% confidence level determined by a t test. Standard curves for each particle type and pH value were made by serial dilutions around the concentrations that passed through the membrane. Using linear

regression, the background-corrected fluorescence from the filtration experiments was then used to calculate concentrations.

Received: November 23, 2009
Revised: January 23, 2010
Published online: February 22, 2010

Keywords: compressibility · gels · hydrogel particles · membranes · renal clearance

[1] T. K. Jain, M. K. Reddy, M. A. Morales, D. L. Leslie-Pelecky, V. Labhasetwar, *Mol. Pharm.* **2008**, *5*, 316.
[2] P. Jie, S. S. Venkatraman, F. Min, B. Y. C. Freddy, G. L. Huat, *J. Controlled Release* **2005**, *110*, 20.
[3] K. Shirota, Y. Kato, K. Suzuki, Y. Sugiyama, *J. Pharmacol. Exp. Ther.* **2001**, *299*, 459.
[4] T. Tabata, Y. Murakami, Y. Ikada, *J. Controlled Release* **1998**, *50*, 123.
[5] X. X. He, H. L. Nie, K. M. Wang, W. H. Tan, X. Wu, P. F. Zhang, *Anal. Chem.* **2008**, *80*, 9597.
[6] M. L. Schipper, G. Iyer, A. L. Koh, Z. Cheng, Y. Ebenstein, A. Aharoni, S. Keren, L. A. Bentolila, J. Q. Li, J. H. Rao, X. Y. Chen, U. Banin, A. M. Wu, R. Sinclair, S. Weiss, S. S. Gambhir, *Small* **2009**, *5*, 126.
[7] C. S. Chen, M. Mrksich, S. Huang, G. M. Whitesides, D. E. Ingber, *Science* **1997**, *276*, 1425.
[8] A. J. Engler, M. A. Griffin, S. Sen, C. G. Bonnetnann, H. L. Sweeney, D. E. Discher, *J. Cell Biol.* **2004**, *166*, 877.
[9] A. J. Engler, S. Sen, H. L. Sweeney, D. E. Discher, *Cell* **2006**, *126*, 677.
[10] H. Shen, J. Tan, W. M. Saltzman, *Nat. Mater.* **2004**, *3*, 569.
[11] D. E. Ingber, *FASEB J.* **2006**, *20*, 811.
[12] S. Mitragotri, J. Lahann, *Nat. Mater.* **2009**, *8*, 15.
[13] K. A. Beningo, Y. L. Wang, *J. Cell Sci.* **2002**, *115*, 849.
[14] X. Banquy, F. Suarez, A. Argaw, J. M. Rabanel, P. Grutter, J. F. Bouchard, P. Hildgen, S. Giasson, *Soft Matter* **2009**, *5*, 3984.
[15] M. E. Fox, F. C. Szoka, J. M. J. Frechet, *Acc. Chem. Res.* **2009**, *42*, 1141.
[16] A. E. Nel, L. Madler, D. Velegol, T. Xia, E. M. V. Hoek, P. Somasundaran, F. Klaessig, V. Castranova, M. Thompson, *Nat. Mater.* **2009**, *8*, 543.
[17] D. Asgeirsson, D. Venturoli, B. Rippe, C. Rippe, *Am. J. Physiol. Renal Physiol.* **2006**, *291*, F1083.
[18] W. M. Deen, M. J. Lazzara, B. D. Myers, *Am. J. Physiol. Renal Physiol.* **2001**, *281*, F579.
[19] C. Rippe, A. Rippe, O. Torffvit, B. Rippe, *Am. J. Physiol. Renal Physiol.* **2007**, *293*, F1533.
[20] A. H. J. Salmon, I. Toma, A. Sipos, P. R. Muston, S. J. Harper, D. O. Bates, C. R. Neal, J. Peti-Peterdi, *Am. J. Physiol. Renal Physiol.* **2007**, *293*, F1777.
[21] C. Lau, I. Sudbury, M. Thomson, P. L. Howard, A. B. Magil, W. A. Cupples, *Am. J. Physiol. Regul. Integr. Comp. Physiol.* **2009**, *296*, R1761.
[22] S. Atzet, S. Curtin, P. Trinh, S. Bryant, B. Ratner, *Biomacromolecules* **2008**, *9*, 3370.
[23] N. Hua, J. Sun, *J. Mater. Sci. Mater. Med.* **2008**, *19*, 3243.
[24] J. H. Park, L. Gu, G. von Maltzahn, E. Ruoslahti, S. N. Bhatia, M. J. Sailor, *Nat. Mater.* **2009**, *8*, 331.
[25] T. S. Troutman, J. K. Barton, M. Romanowski, *Adv. Mater.* **2008**, *20*, 2604.
[26] H. S. Choi, W. Liu, P. Misra, E. Tanaka, J. P. Zimmer, B. I. Ipe, M. G. Bawendi, J. V. Frangioni, *Nat. Biotechnol.* **2007**, *25*, 1165.
[27] C. P. Parungo, D. I. Soybel, Y. L. Colson, S. W. Kim, S. Ohnishi, A. M. DeGrand, R. G. Laurence, E. G. Soltesz, F. Y. Chen, L. H. Cohn, M. G. Bawendi, J. V. Frangioni, *Ann. Surg. Oncol.* **2007**, *14*, 286.
[28] A. S. Iyer, L. A. Lyon, *Angew. Chem.* **2009**, *121*, 4632; *Angew. Chem. Int. Ed.* **2009**, *48*, 4562.
[29] T. R. Matzelle, G. Geuskens, N. Kruse, *Macromolecules* **2003**, *36*, 2926.
[30] Z. Meng, J. K. Cho, V. Breedveld, L. A. Lyon, *J. Phys. Chem. B* **2009**, *113*, 4590.
[31] Z. Y. Meng, J. K. Cho, S. Debord, V. Breedveld, L. A. Lyon, *J. Phys. Chem. B* **2007**, *111*, 6992.
[32] A. N. St. John, V. Breedveld, L. A. Lyon, *J. Phys. Chem. B* **2007**, *111*, 7796.
[33] W. H. Blackburn, L. A. Lyon, *Colloid Polym. Sci.* **2008**, *286*, 563.
[34] W. H. Fissell, S. Manley, A. Dubnisheva, J. Glass, J. Magistrelli, A. N. Eldridge, A. J. Fleischman, A. L. Zydney, S. Roy, *Am. J. Physiol. Renal Physiol.* **2007**, *293*, F1209.
[35] G. A. Tanner, C. Rippe, Y. Z. Shao, A. P. Evan, J. C. Williams, *Am. J. Physiol. Renal Physiol.* **2009**, *296*, F1269.
[36] P. G. de Gennes in *Polymers in Confined Environments*, *Vol. 138*, Springer, Berlin, **1999**, p. 91.
[37] M. Muthukumar, *Phys. Rev. Lett.* **2001**, *86*, 3188.
[38] M. I. Papisov, *Adv. Drug Delivery Rev.* **1995**, *16*, 127.
[39] C. T. A. Wong, M. Muthukumar, *Biophys. J.* **2008**, *95*, 3619.
[40] C. T. A. Wong, M. Muthukumar, *J. Chem. Phys.* **2008**, *128*, 154903.
[41] M. J. Serpe, C. D. Jones, L. A. Lyon, *Langmuir* **2003**, *19*, 8759.
[42] J. D. Debord, L. A. Lyon, *J. Phys. Chem. B* **2000**, *104*, 6327.
[43] Y. D. Yi, Y. C. Bae, *J. Appl. Polym. Sci.* **1998**, *67*, 2087.

